International Journal of Heat and Mass Transfer 215 (2023) 124475

Contents lists available at ScienceDirect

International Journal of Heat and Mass Transfer

journal homepage: www.elsevier.com/locate/ijhmt

Four-phonon and normal scattering in 2D hexagonal structures

Guoqing Sun[a], Jinlong Ma[a], Chenhan Liu[b], Zheng Xiang[a], Dongwei Xu[a,*], Te-Huan Liu[a], Xiaobing Luo[a]

[a] State Key Laboratory of Coal Combustion, School of Energy and Power Engineering, Huazhong University of Science and Technology, Wuhan,430074, China
[b] Micro- and Nano-scale Thermal Measurement and Thermal Management Laboratory, School of Energy and Mechanical Engineering, Nanjing Normal University, Nanjing, 210023, China

ARTICLE INFO

Article history:
Received 24 February 2023
Revised 2 June 2023
Accepted 2 July 2023

Keywords:
Four-phonon
Normal scattering
Scattering rate
Thermal conductivity

ABSTRACT

Comprehensive understanding of phonon transport will facilitate the exploration of materials. Four-phonon scattering is find to be important to determine thermal conductivity in many materials, and normal scattering (N process) could lead to some unique phonon transport behaviors, especially in 2D materials. In this work, we studied four-phonon and normal scattering in hexagonal structures, both of which were found to be significant. With the increase of atomic mass ratio, the relative four-phonon scattering is gradually enhanced, whereas N process is weakened. Callaway model and Allen's modified models were used to approximate the thermal conductivity, and we find that the models are applicable in some cases with relative weak N scattering intensity.

1. Introduction

Due to the novel properties of two-dimensional (2D) materials and the progress of nanotechnology, two-dimensional materials are receiving increasing attention. 2D materials provide an ideal platform to explore the various phonon behaviors. For example, graphene has the highest thermal conductivity to date [1,2] and a lot of researches have been devoted to understanding phonon transport in it [3,4].

The exact thermal conductivity of graphene has been explored a lot. For example, Zou et al. have found that the performance of MD simulation on thermal conductivity of graphene greatly depends on the potential used [3]. As a method without adjustable parameters, there is no doubt that three-phonon based phonon Boltzmann transport calculation has gained great success in predicting phonon properties [5–7], however, some studies have shown that considering three-phonon alone is insufficient to fully understand phonon properties. Feng et al. found that the length-dependent thermal conductivity of 9 μm graphene is reduced from 3383 to ~810 W/(mK) at room temperature by involving four-phonon scattering [8], indicating the significant effect of four-phonon process. It has been proved that four-phonon scattering is generally important in some solids and can remedy the discrepancies between experiment and calculation values [9–12]. And in particular, the inclusion of four-phonon scattering reduces the room-temperature thermal conductivity of BAs and AlSb by 48% and 70% respectively, indicating that four-phonon scattering is more important than three-phonon scattering [10] in these materials. In more studies involving four-phonon scattering [13–17], the decrease in thermal conductivity of 2D materials has ranged from ~40% to ~90%.

Graphene's ultra-high thermal conductivity has been attributed to the strong normal scattering [18–22]. Normal (N) and Umklapp (U) scattering are defined regarding the momentum conservation [23]. In the N process, the total momentum of phonon is conserved: $\vec{q_1} + \vec{q_2} = \vec{q_3}$, hence, N process does not contribute directly to thermal resistance but it could affect phonon transport by redistributing the phonon momentum. For the U process, the net momentum changes: $\vec{q_1} + \vec{q_2} = \vec{q_3} + \Delta\vec{G}$. It creates a phonon with a momentum k-vector outside the first BZ. And the phonon propagation direction is reversed, directly causing thermal resistance. In 2D materials like graphene, the large anharmonicity and density of states of the quadratic ZA mode enhance N process and thus leads to high thermal conductivity [18,20,24]. N scattering is also responsible for other interesting phenomena, such as strong size effect [25,26], Poiseuille flow [27–29], and second sound [29,30]. Moreover, thermal transport can be enhanced by modulating N/U scattering in materials like bilayer graphene [31].

From the above literature review, it can be seen that the exploration of the four-phonon as well as N/U scattering is important for understanding phonon transport. However, when those effects should be considered in the calculation of thermal transport, and, how significant are the effects remain to be explored. Here we se-

* Corresponding author.
E-mail addresses: dwxu@hust.edu.cn (D. Xu), thliu@hust.edu.cn (T.-H. Liu).

https://doi.org/10.1016/j.ijheatmasstransfer.2023.124475
0017-9310/

Table 1
Comparison of thermal conductivity (in W/(mK)) under 300 K obtained from iteration (ITE), RTA and Callaway and Allen models. The data in parentheses represent deviations from the accurate thermal conductivity (iterative solution). The downward arrows in the column of 3&4 ph ITE represent the magnitude of the reduction in thermal conductivity due to four-phonon scattering, which is the amount of reduction compared to the three-phonon limited iterative solution.

	3ph ITE	3ph RTA	3ph Callaway	3ph Allen	3&4 ph ITE	3&4 ph RTA	3&4 ph Callaway	3&4 ph Allen
Graphene	3058.6	487.8 (-84%)	1241.4 (-59%)	1890.8 (-38%)	1389.5 ↓ 55%	375.3 (-73%)	851.9 (-39%)	810.5 (-42%)
BN	1024.6	242.2 (-76%)	438.7 (-57%)	821.2 (-20%)	229.4 ↓ 78%	165.1 (-28%)	227.1 (-1%)	227.9 (-1%)
AlN	190.1	55.6 (-71%)	74.3 (-61%)	128.8 (-32%)	21.2 ↓ 89%	20.0 (-6%)	20.3 (-4%)	21.1 (0%)
GaN	21.9	11.0 (-50%)	13.4 (-39%)	29.7 (36%)	1.39 ↓ 94%	1.36 (-2%)	1.37 (-1%)	1.41 (1%)

lect a series of simplest planar hexagonal structures, graphene-like materials, to study the atomic ratio effect on the four-phonon and N/U scattering process, where the influencing factor of structure has been equally treated. In this study, we have investigated the four-phonon and N/U scattering in graphene and XN (X = B, Al, Ga) by means of first-principles combined with phonon Boltzmann transport equation (BTE). The calculations show that four-phonon scattering plays a significant role in all the four considered materials and the relative four-phonon scattering is gradually enhanced with the increasing of atomic ratio, while the relative N scattering intensity decreases.

2. Computational details

The first principle calculations are carried out employing the Vienna *ab initio* simulation package (VASP). The Perdew-Burke-Ernzerhof (PBE) generalized gradient approximation (GGA) is adopted as the exchange-correlation functional. All the four structures (graphene, BN, AlN, and GaN) use a plane wave basis with a cutoff energy of 600 eV, and the Brillouin zone (BZ) is sampled using 18 × 18×1 Γ-centered k-mesh grids. A vacuum spacing with the thickness of 20 Å is used to avoid the effect of mirror interaction.

Thermal conductivity is obtained by the Boltzmann transport equation solver FourPhonon program [32]. In the scheme of phonon BTE, the thermal conductivity can be written as [33]:

$$k^{\alpha\beta} = \frac{1}{k_B T^2 8\pi^3} \sum_{\lambda} \int (f_0^2 + f_0)\hbar^2 \omega_{\lambda,q}^2 v_{\lambda,q}^{\alpha} v_{\lambda,q}^{\beta} \tau_{\lambda,q} dq \quad (1)$$

where f_0 is phonon distribution function, ω is phonon frequency and is obtained by diagonalizing the dynamic matrix. Phonon branch and wave vector are represented by λ and $\mathbf{q}$, respectively. α, β are Cartesian directions. τ and v represent phonon lifetime and group velocity respectively, which are usually decisive for thermal conductivity.

Force constants (IFCs) are required to solve BTE. All the force constants are calculated using real-space finite-difference method with 5 × 5×1 supercells, and BZs are sampled with only the Γ point. 7th and 3rd nearest neighboring atoms are considered when calculating the 3rd and 4th IFCs. And in order to get the convergence of the thermal conductivity, the integration of BZs are sampled with a q-mesh of 140 × 140×1 and 40 × 40× for only three- and four-phonon included processes, respectively. And the convergence test for the parameters can be found in the supporting information.

Relaxation time approximation (RTA) is conventionally employed to solve the BTE problem. However, RTA treats both N and U processes as thermal resistance, resulting in an underestimation of the intrinsic thermal conductivity in the N dominated system. Starting from the RTA solution, an iterative process (ITE) can be made to obtain an exact thermal conductivity. Iteration on three-phonon process can be made with ShengBTE package, and for four-phonon scattering, we use our in-house modified ShengBTE code to perform the iteration process when four-phonon scattering is included.

3. Results and discussion

3.1. Four-phonon scattering

The thermal conductivity involving only three-phonon scattering at 300 K for graphene, BN, and GaN is 3058.6, 1024.6, and 21.9 W/(mK) (also shown in Table 1), respectively, which is consistent with literature results [31,34–37]. For AlN, we obtained a thermal conductivity of 190.1 W/(mK), which is higher than the result of *Wang* et al. (73.4 W/(mK)) [38], however, lower than that of *Banerjee* et al. (306.5 W(mK)) [39]. The difference may origin from the larger cutoff neighbor and q-mesh in this work. The calculated four-phonon thermal conductivity is 1389.5, 229.4, 21.2 and 1.39 W/(mK) for graphene, BN, AlN, and GaN, all of which show significant decrease compared to the three-phonon limited thermal conductivity. Our four-phonon thermal conductivity of graphene is higher than that of Feng et al. [8], however, as Feng et al. have declared, since the 4th IFCs in their work is obtained using classical interatomic potential and has not been validated against first principles, the absolute value of thermal conductivity after including four-phonon scattering should be interpreted qualitatively.

We plot the phonon spectrum in Fig. S4. Band gaps of 4.9 and 9.9 THz are found in AlN and GaN, respectively, which stem from the large atomic mass ratio (1.9 for AlN and 4.4 for GaN). In materials like 2D BAs [13], bulk BAs [9], and NbC [40], large phonon band gaps limit the three-phonon processes, however, it is not a restriction for four-phonon processes, thus lead to significant four-phonon scattering phase space. We further plot the phase space [41] of three- and four-phonon scattering process in Fig. S5. The phase space of three-phonon is more significant in graphene and BN while it is relatively weakened in AlN and GaN. It is hard to satisfy energy conservation in three-phonon scattering process due to the large phonon band gap, however, it does not limit the four-phonon processes between the upper and lower branches. Therefore, the three-phonon scattering phase space of the acoustic branch's high frequency phonons of GaN is comparable to that of four-phonon (as marked in the red ellipse in Fig. S5 (d)). The scattering phase space is also decomposed into three individual processes, namely, splitting (three-phonon process: $\lambda_1 \rightarrow \lambda_2 + \lambda_3$, four-phonon process: $\lambda_1 \rightarrow \lambda_2 + \lambda_3 + \lambda_4$), recombination (the reverse of the splitting process) and redistribution (four-phonon process: $\lambda_1 + \lambda_2 \rightarrow \lambda_3 + \lambda_4$). The three processes shown in Fig. S6 and S7 indicate that the phase space of splitting process increases with the increase of phonon frequency. At low-frequency region, the splitting process is limited due to the lack of quantum state accepting the emitted phonon and thus the energy conservation can not be satisfied. In contrast, phase space of recombination process decreases with the increase of frequency. Correspondingly, the cause is the lack of states that accept the combined phonon. In particular for four-phonon scattering, phase space is dominated by the redistribution process.

The ratio of scattering rate of four-phonon to three-phonon process is shown in Fig. 1 to reveal the importance of four-phonon scattering. In graphene, three-phonon scattering rate is larger than four-phonon, however, with the increase of atomic mass ratio, ra-

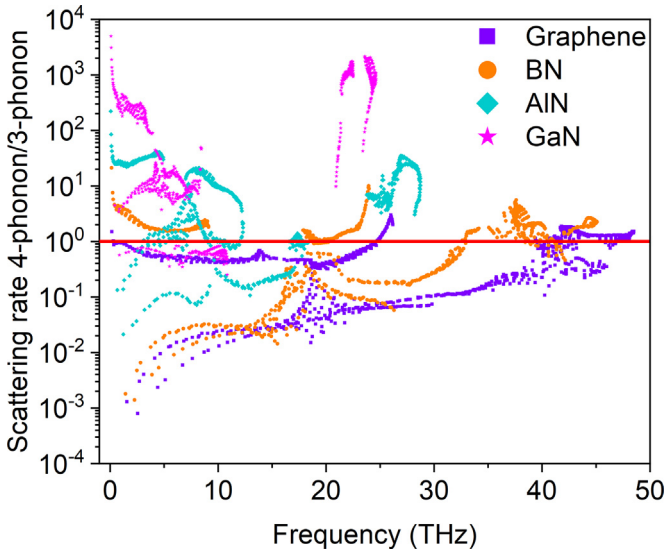

Fig. 1. The ratio of scattering rate of four-phonon to three-phonon, which is used to characterize the relative four-phonon scattering intensity. The horizon red line marks the equal proportion ratio. (For interpretation of the references to colour in this figure legend, the reader is referred to the web version of this article.)

tio of scattering rate of four-phonon to three phonon begins to be greater than 1 and shows an increasing trend. This means that four-phonon scattering contributes an increasing amount of thermal resistance, as a result, when four-phonon scattering events are involved, the thermal conductivity decreases 55%, 78%, 89% and 94% for graphene, BN, AlN and GaN respectively compared with the results including three-phonon scattering only. Comparison between the mean free path with and without considering four-phonon scattering is shown in Fig. S8, it can be found that the mean free path is significantly shortened for all four materials by four-phonon scattering, with GaN the most shortened. The above analysis shows that with the increase of atomic mass ratio, the importance of four-phonon scattering increases, and the corresponding reduction in thermal conductivity due to four-phonon scattering becomes more pronounced.

To gain a deeper insight into the phonon scattering mechanism, we decompose the phonon scattering rate into different channels in Fig. 2. It is clear that the suppression of thermal conductivity by four-phonon scattering is caused mostly by the scattering event involving four acoustic phonons, and the increase in atomic mass ratio enhances *aaaa* channel. Feng has attributed the surprisingly high four acoustic phonons scattering in graphene to the fact that the reflection symmetry allows significantly more four-phonon processes than three-phonon processes [8]. Here we have proved that high four-phonon scattering rate also exist in other three planar 2D materials, and as the atomic mass ratio raises, four acoustic phonons scattering becomes increasingly important.

3.2. Normal scattering

To explore the N and U scattering in those four materials, we decompose the scattering rate into N and U processes, and the ratio of the two is shown in Fig. 3. In general, N scattering is dom-

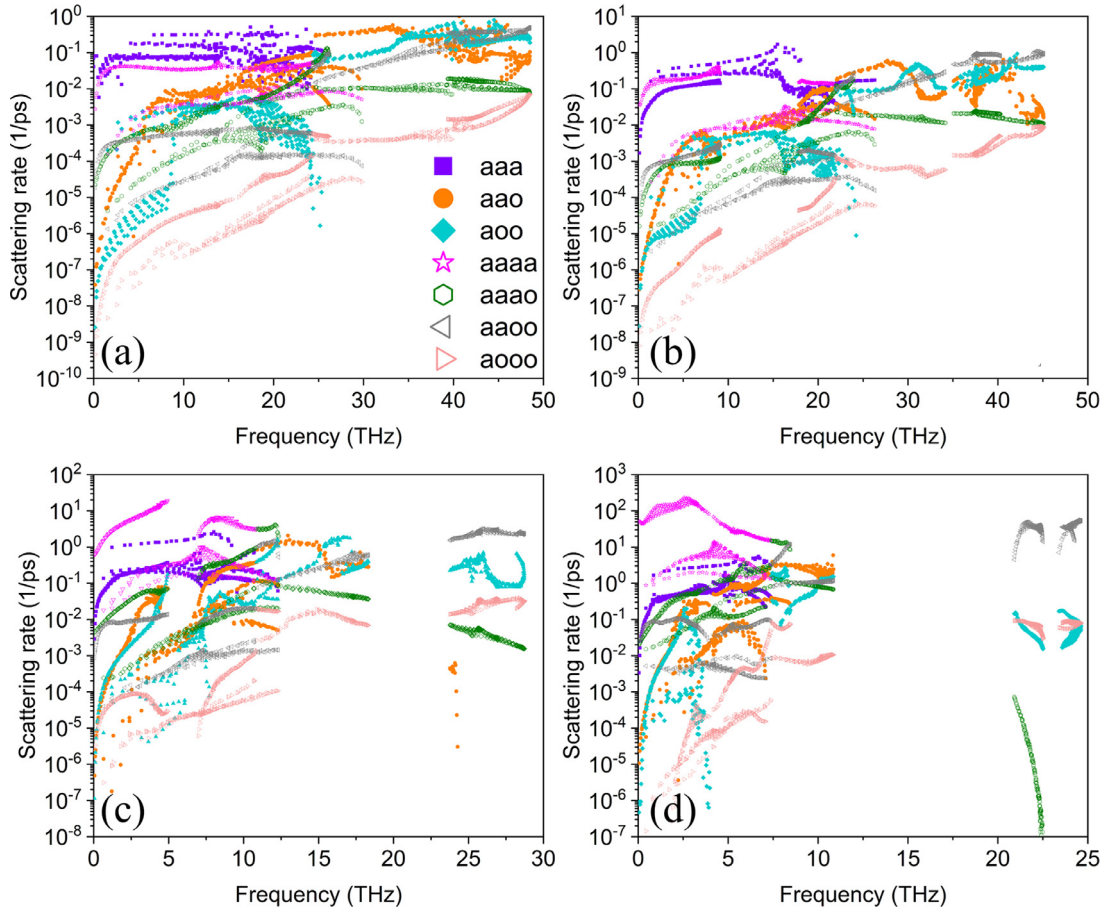

Fig. 2. Decomposed scattering rate of (a) graphene, (b) BN, (c) AlN, and (d) GaN. The letter a represents for acoustic phonon, and o is optical phonon, e.g., aaa stands for the scattering event involving three acoustic phonons, and aaaa represents scattering involving four acoustic phonons.

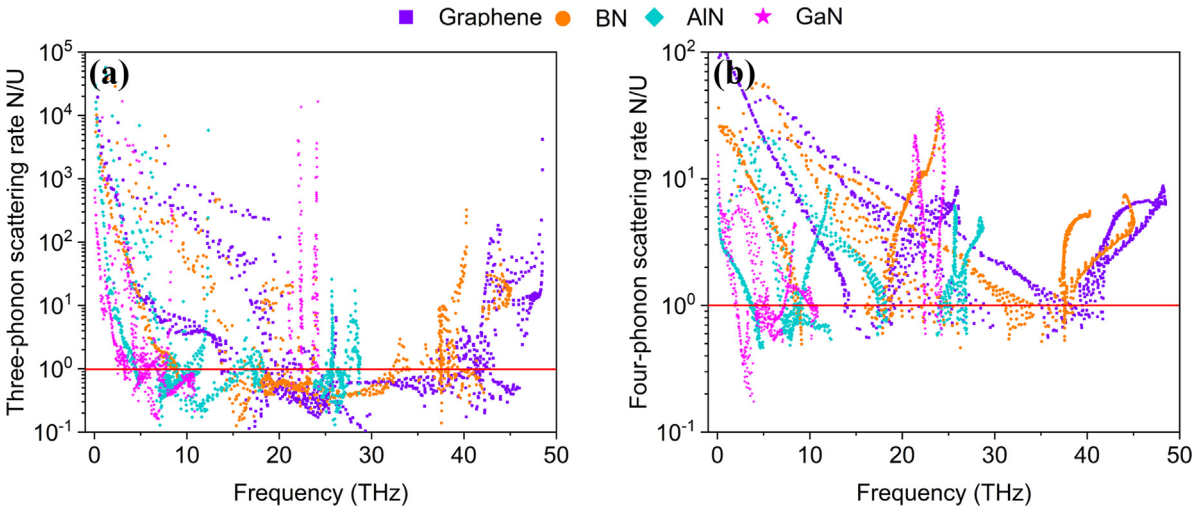

Fig. 3. The ratio of scattering rate of N process to U process (N/U) in (a) three-phonon and (b) four-phonon scattering process, which is used to characterized the normal scatering intensity. Horizon red lines mark the equal proportion ratio.

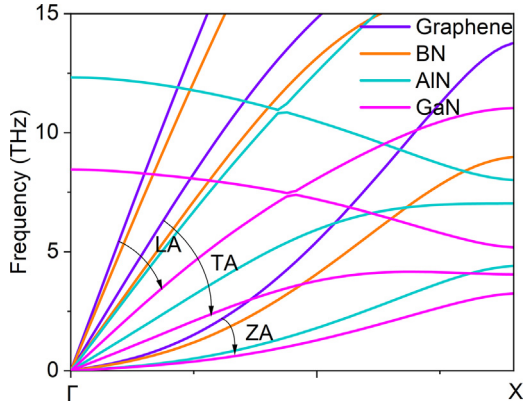

Fig. 4. Local phonon spectrum of graphene, BN, AlN, and GaN, and the black arrows show the trends of phonon branches.

inant in both three- and four-phonon scattering, and is more significant in three-phonon process. The reason is that, with the invloving of an additional phonon, four-phonon scattering is easier to create a phonon with a momentum beyond the first BZ, and thus weakens N process. Another interesting phenomenon is that with the sequence of graphene, BN, AlN, GaN (increasing of atomic ratio), the N process gradually weakens, although it is still dominant. The reason can be found in the local phonon spectrum as shown in Fig. 4. The population of phonon obeys the Bose-Einstein distribution [8], and in this dependence, low frequency modes have much more phonons than high frequency modes and they significantly affect thermal transport properties. In graphene, the noteworthy strong N scattering has been attributed to its high Debye temperature, quadratic phonon band and diverging Grüneisen parameter [42], the latter two of which are common to planar 2D structures. As atomic ratio increases, the phonon branches are softened to lower frequency (as shown in Fig. 4), and the Debye temperature decreases correspondingly. It means that, at typical temperatures of interest, the phonon distribution will be more in states away from the Γ point, and the low-lying branches makes phonons have larger wave vectors and have more possibilities to scatter outside the first BZ, which leads to the weakening of N scattering event in three- and four-phonon process. The Grüneisen parameter is calculated and shown in Fig. S9. Grüneisen parameter diverges and gets a large magnitude near the BZ center, and larger Grüneisen parameter appears in AlN and GaN; however, the aforementioned lowering of the phonon branches is more important, resulting in the weakening of relative N scattering intensity with the rising atomic mass ratio.

In addition, given that the iterative solution is obtained, we can compare the strength of the N scattering through the deviation between the iterative solution and RTA solution. As indicated in Table 1, three-phonon limited thermal conductivity obtained by the RTA method is 487.8 W/(mK), 242.2 W/(mK), 55.6 W/(mK), and 11.0 W/(mK) at 300K for graphene, BN, AlN and GaN respectively, which are 84%, 76%, 71%, and 50% lower than those obtained by iterative method. Such large differences imply that N process play an important role in three-phonon scattering process and its effect decreases with the atomic ratio. When four-phonon scattering is included in calculating the thermal conductivity, the deviations of the two results are -73%, -28%, -6% and -2% for graphene, BN, and AlN, and GaN. The smaller deviations compared with those in three-phonon process stem from the joint contribution of two factors: (a) the importance of four-phonon scattering makes the treatment on it has significant impact on the result, and (b) the weaker relative N scattering intensity in four-phonon process, making the difference between the iterative and RTA solutions increasingly smaller.

3.3. Model approximation

The fact that exact solutions to thermal conductivity have been obtained allows us to test the efficacy of the two widely used approaches: Callaway and Allen models [43–47]. As we have discussed in Section 2, N scattering does not directly provide thermal resistance, an identical treatment of N and U process by RTA method would lead to an underestimation of thermal conductivity. Callaway model is proposed to compensate for this underestimation [48], by treating N and U scattering differently. Allen proposed a modified Callaway by using a different constraint condition imposed by the N scattering [49]. More details about Callaway and Allen models can be found in the Supporting Information. Hereby, we conduct an examination of the accuracy of the Callaway model and Allen's modified version with three- and four-phonon process, and the results are shown in Table 1. It can be found that in the framework of three-phonon scattering, thermal conductivity of all four materials is significantly underestimated by the RTA method, and the Callaway and Allen models make up for part of the underestimation. The deviations of the Callaway model from the itera-

tive solution are -59%, -57%, -61%, -39% for graphene, BN, AlN, and GaN, respectively, while that of Allen's model are -38%, -20%, -32%, and 36%, both models deviate less compared to the RTA, with the Allen model having smaller deviations, although the accuracy can not guaranteed.

When four-phonon scattering is included, the underestimations by RTA are reduced. Similar to three-phonon limited thermal conductivity, the two models show better performance than RTA. In addition, it is found that the two models' deviations are less than 5% in BN, AlN, and GaN, implying that both the Callaway and Allen models can guarantee the accuracy in those three materials. For graphene, the deviations of two models are still as large as -39% and -42% respectively, although there is a significant improvement over RTA method. The inaccurate approximation to graphene may stem from the strongest N scattering among those four materials.

4. Conclusion

Based on first principles calculation combined BTE, four-phonon and normal scattering in graphene, BN, AlN, and GaN are explored. Due to the increasingly important role of *aaaa* scattering channel, four-phonon scattering is found to have great effects on all the four materials, which results in reductions of three-phonon limited thermal conductivity of 55%, 78%, 89% and 94%, respectively. N process is much stronger in three-phonon process than that in four-phonon process, which is attributed to the participation of an additional phonon and it should exist in other materials as well. The increase of atomic mass ratio will enhance four-phonon scattering, but conversely, will weaken relative N scattering intensity. Additionally, we examined the accuracy of the Callaway model and Allen's modified version, it is found that neither model is applicable in three-phonon limited process with strong N scattering. In the cases where four-phonon scattering is included, both models could guarantee the accuracy of thermal conductivity in BN, AlN and GaN, for graphene, however, N scattering is still too significant to be well described by the models.

Declaration of Competing Interest

The authors declare that they have no known competing financial interests or personal relationships that could have appeared to influence the work reported in this paper.

CRediT authorship contribution statement

Guoqing Sun: Conceptualization, Methodology, Visualization, Investigation, Writing – original draft. **Jinlong Ma:** Methodology, Investigation. **Chenhan Liu:** Methodology, Investigation. **Zheng Xiang:** Resources, Supervision. **Dongwei Xu:** Methodology, Conceptualization, Funding acquisition, Resources, Supervision, Writing – review & editing. **Te-Huan Liu:** Methodology, Software, Validation, Writing – review & editing. **Xiaobing Luo:** Supervision, Project administration.

Data availability

Data will be made available on request.

Acknowledgments

D. X. acknowledges the support from the National Natural Science Foundation of China (No. 51806072). J. M. acknowledges the support from National Key Research and Development Program of China (No. 2022YFC2204400). T.-H. L. acknowledges the support from the National Natural Science Foundation of China (No. 52076089). And this work is supported by the zhonghe II supercomputer in the Jiangsu Century-horizon Information Technology Co, Ltd at Nanjing.

Supplementary material

Supplementary material associated with this article can be found, in the online version, at 10.1016/j.ijheatmasstransfer.2023.124475.

References

[1] A.A. Balandin, S. Ghosh, W. Bao, I. Calizo, D. Teweldebrhan, F. Miao, C.N. Lau, Superior thermal conductivity of single-layer graphene, Nano Lett. 8 (3) (2008) 902–907.
[2] D.S. Ghosh, I. Calizo, D. Teweldebrhan, E.P. Pokatilov, D.L. Nika, A.A. Balandin, W. Bao, F. Miao, C.N. Lau, Extremely high thermal conductivity of graphene: prospects for thermal management applications in nanoelectronic circuits, Appl. Phys. Lett. 92 (15) (2008) 151911.
[3] J.-H. Zou, Z.-Q. Ye, B.-Y. Cao, Phonon thermal properties of graphene from molecular dynamics using different potentials, J. Chem. Phys. 145 (13) (2016) 134705.
[4] J.-H. Zou, B.-Y. Cao, Phonon thermal properties of graphene on h-BN from molecular dynamics simulations, Appl. Phys. Lett. 110 (10) (2017) 103106.
[5] L. Lindsay, C. Hua, X.L. Ruan, S. Lee, Survey of ab initio phonon thermal transport, Mater. Today Phys. 7 (2018) 106–120.
[6] Y. Quan, S. Yue, B. Liao, Impact of electron-phonon interaction on thermal transport: a review, Nanoscale Microscale Thermophys. Eng. 25 (2) (2021) 73–90.
[7] X. Yan, B. Wang, Y. Hai, D.R. Kripalani, Q. Ke, Y. Cai, Phonon anharmonicity and thermal conductivity of two-dimensional van der Waals materials: a review, Sci. China Phys. Mech. Astron. 65 (11) (2022) 117004.
[8] T. Feng, X. Ruan, Four-phonon scattering reduces intrinsic thermal conductivity of graphene and the contributions from flexural phonons, Phys. Rev. B 97 (4) (2018) 045202.
[9] T. Feng, L. Lindsay, X. Ruan, Four-phonon scattering significantly reduces intrinsic thermal conductivity of solids, Phys. Rev. B 96 (16) (2017) 161201.
[10] X. Yang, T. Feng, J. Li, X. Ruan, Stronger role of four-phonon scattering than three-phonon scattering in thermal conductivity of III-V semiconductors at room temperature, Phys. Rev. B 100 (24) (2019) 245203.
[11] L. Xie, J.H. Feng, R. Li, J.Q. He, First-principles study of anharmonic lattice dynamics in low thermal conductivity agcrse 2: evidence for a large resonant four-phonon scattering, Phys. Rev. Lett. 125 (24) (2020) 245901.
[12] X. Gu, S. Li, H. Bao, Thermal conductivity of silicon at elevated temperature: role of four-phonon scattering and electronic heat conduction, Int. J. Heat Mass Transf. 160 (2020) 120165.
[13] C. Yu, Y. Hu, J. He, S. Lu, D. Li, J. Chen, Strong four-phonon scattering in monolayer and hydrogenated bilayer BAs with horizontal mirror symmetry, Appl. Phys. Lett. 120 (13) (2022) 132201.
[14] C. Zhang, J. Sun, Y. Shen, W. Kang, Q. Wang, Effect of high order phonon scattering on the thermal conductivity and its response to strain of a penta-NiN2 sheet, J. Phys. Chem. Lett. 13 (25) (2022) 5734–5741.
[15] Y. Zhang, Z. Tong, A. Pecchia, C. Yam, T. Dumitrică, T. Frauenheim, Four-phonon and electron–phonon scattering effects on thermal properties in two-dimensional 2H-TaS2, Nanoscale 14 (36) (2022) 13053–13058.
[16] T. Li, P.-H. Du, L. Bai, Q. Sun, P. Jena, et al., NaNO 3 monolayer: a stable graphenelike supersalt with strong four-phonon scattering and low lattice thermal conductivity insensitive to temperature, Phys. Rev. Mater. 6 (6) (2022) 064009.
[17] J. Sun, C. Zhang, Z. Yang, Y. Shen, M. Hu, Q. Wang, Four-phonon scattering effect and two-channel thermal transport in two-dimensional paraelectric SnSe, ACS Appl. Mater. Interfaces 14 (9) (2022) 11493–11499.
[18] J.H. Seol, I. Jo, A.L. Moore, L. Lindsay, Z.H. Aitken, M.T. Pettes, X. Li, Z. Yao, R. Huang, D. Broido, et al., Two-dimensional phonon transport in supported graphene, Science 328 (5975) (2010) 213–216.
[19] D.L. Nika, A.A. Balandin, Phonons and thermal transport in graphene and graphene-based materials, Rep. Prog. Phys. 80 (3) (2017) 036502.
[20] L. Lindsay, D.A. Broido, N. Mingo, Flexural phonons and thermal transport in graphene, Phys. Rev. B 82 (11) (2010) 115427.
[21] A.A. Balandin, Phononics of graphene and related materials, ACS Nano 14 (5) (2020) 5170–5178.
[22] C. Liu, P. Lu, W. Chen, Y. Zhao, Y. Chen, Phonon transport in graphene based materials, Phys. Chem. Chem. Phys. 23 (46) (2021) 26030–26060.
[23] Z. Chen, X. Zhang, Y. Pei, Manipulation of phonon transport in thermoelectrics, Adv. Mater. 30 (17) (2018) 1705617.
[24] N. Bonini, J. Garg, N. Marzari, Acoustic phonon lifetimes and thermal transport in free-standing and strained graphene, Nano Lett. 12 (6) (2012) 2673–2678.
[25] G. Chen, Non-fourier phonon heat conduction at the microscale and nanoscale, Nat. Rev. Phys. 3 (8) (2021) 555–569.
[26] V.A. Cimmelli, A. Sellitto, D. Jou, Nonlinear evolution and stability of the heat flow in nanosystems: beyond linear phonon hydrodynamics, Phys. Rev. B 82 (18) (2010) 184302.

[27] Y. Machida, A. Subedi, K. Akiba, A. Miyake, M. Tokunaga, Y. Akahama, K. Izawa, K. Behnia, Observation of poiseuille flow of phonons in black phosphorus, Sci. Adv. 4 (6) (2018) eaat3374.
[28] X. Huang, Y. Guo, Y. Wu, S. Masubuchi, K. Watanabe, T. Taniguchi, Z. Zhang, S. Volz, T. Machida, M. Nomura, Observation of phonon poiseuille flow in isotopically purified graphite ribbons, Nat. Commun. 14 (1) (2023) 2044.
[29] R.A. Guyer, J.A. Krumhansl, Thermal conductivity, second sound, and phonon hydrodynamic phenomena in nonmetallic crystals, Phys. Rev. 148 (2) (1966) 778.
[30] H.E. Jackson, C.T. Walker, Thermal conductivity, second sound, and phonon-phonon interactions in NaF, Phys. Rev. B 3 (4) (1971) 1428.
[31] F. Duan, C. Shen, H. Zhang, G. Qin, Hydrodynamically enhanced thermal transport due to strong interlayer interactions: a case study of strained bilayer graphene, Phys. Rev. B 105 (12) (2022) 125406.
[32] Z. Han, X. Yang, W. Li, T. Feng, X. Ruan, FourPhonon: an extension module to shengBTE for computing four-phonon scattering rates and thermal conductivity, Comput. Phys. Commun. 270 (2022) 108179.
[33] G. Sun, Y. Cheng, J. Ma, D. Xu, X. Luo, Strain effect on the phonon transport properties of hydrogenated 2D GaN, Vacuum (2023) 111808.
[34] G. Qin, Z. Qin, H. Wang, M. Hu, Anomalously temperature-dependent thermal conductivity of monolayer GaN with large deviations from the traditional 1/T law, Phys. Rev. B 95 (19) (2017) 195416.
[35] Z. Qin, G. Qin, X. Zuo, Z. Xiong, M. Hu, Orbitally driven low thermal conductivity of monolayer gallium nitride (GaN) with planar honeycomb structure: a comparative study, Nanoscale 9 (12) (2017) 4295–4309.
[36] H. Fan, H. Wu, L. Lindsay, Y. Hu, Ab initio investigation of single-layer high thermal conductivity boron compounds, Phys. Rev. B 100 (8) (2019) 085420.
[37] Y. Kuang, L. Lindsay, B. Huang, Unusual enhancement in intrinsic thermal conductivity of multilayer graphene by tensile strains, Nano Lett. 15 (9) (2015) 6121–6127.
[38] H. Wang, L. Yu, J. Xu, D. Wei, G. Qin, Y. Yao, M. Hu, Intrinsically low lattice thermal conductivity of monolayer hexagonal aluminum nitride (h-ALN) from first-principles: acomparative study with graphene, Int. J. Therm. Sci. 162 (2021) 106772.
[39] A. Banerjee, B.K. Das, K.K. Chattopadhyay, Significant enhancement of lattice thermal conductivity of monolayer ALN under bi-axial strain: a first principles study, Phys. Chem. Chem. Phys. 24 (26) (2022) 16065–16074.
[40] C. Li, N.K. Ravichandran, L. Lindsay, D. Broido, Fermi surface nesting and phonon frequency gap drive anomalous thermal transport, Phys. Rev. Lett. 121 (17) (2018) 175901.
[41] W. Li, N. Mingo, Ultralow lattice thermal conductivity of the fully filled skutterudite YbFe4Sb12 due to the flat avoided-crossing filler modes, Phys. Rev. B 91 (14) (2015) 144304.
[42] S. Lee, D. Broido, K. Esfarjani, G. Chen, Hydrodynamic phonon transport in suspended graphene, Nat. Commun. 6 (1) (2015) 1–10.
[43] Y. Zhang, E. Skoug, J. Cain, V. Ozoliš, D. Morelli, C. Wolverton, First-principles description of anomalously low lattice thermal conductivity in thermoelectric Cu-Sb-Se ternary semiconductors, Phys. Rev. B 85 (5) (2012) 054306.
[44] W. Kim, J. Zide, A. Gossard, D. Klenov, S. Stemmer, A. Shakouri, A. Majumdar, Thermal conductivity reduction and thermoelectric figure of merit increase by embedding nanoparticles in crystalline semiconductors, Phys. Rev. Lett. 96 (4) (2006) 045901.
[45] A. Alofi, G.P. Srivastava, Phonon conductivity in graphene, J. Appl. Phys. 112 (1) (2012) 013517.
[46] A. AlShaikhi, S. Barman, G.P. Srivastava, Theory of the lattice thermal conductivity in bulk and films of GaN, Phys. Rev. B 81 (19) (2010) 195320.
[47] C. Liu, C. Wu, P. Lu, Y. Zhao, Non-monotonic thickness dependent hydrodynamic phonon transport in layered titanium trisulphide: first-principles calculation and improved callaway model fitting, ES Energy Environ. 14 (2021) 34–42.
[48] J. Callaway, Model for lattice thermal conductivity at low temperatures, Phys. Rev. 113 (4) (1959) 1046.
[49] P.B. Allen, Improved callaway model for lattice thermal conductivity, Phys. Rev. B 88 (14) (2013) 144302.